Journal of Engineering and Applied Sciences 13 (22): 9643-9650, 2018
ISSN: 1816-949X


# Non-Linear Analysis of Composite Beam Subjected to Fire

[1]Muhaned A. Shallal and [2]Aqil Mousa K. Al Musawi
[1]Department of Civil Engineering,
[2]Department of Roads and Transports Engineering, Al-Qadisiyah University, Al Diwaniyah, Iraq

**Abstract:** The composite members consist of two materials such as steel and concrete and when flexible joints are used, slip will happening between the two materials. The fires effect has been studied on this type of construction members. Two of the beams were examined, one of them was loaded with concentrated force in the middle of the beam and the second was loaded with uniform distributed. Both beams were exposed to different fire periods of 0, 30, 60, 90, 120, 150, 180 min. The most important conclusions were the failure of one of the beams (Beam No. 2) when exposed to a fire period of up to 180 min. The effect on deflection was clear with the maximum increase in deflection reaching 603% in the first beam and 456% in the second beam. Slip was affected by the exposure of composite beams to fire, with the largest increase of 181 and 152% for the first and second beams, respectively.

**Key words:** Non-linear analysis, fire, composite beam, deflection, slip, partial interaction, stiffness matrix

## INTRODUCTION

The beams produced by a combination of 2 or more elements are called composite beams, to connect these elements (steel and concrete) with some we use what is known as the shear connectors, the composite beams are capable of resisting bending moments and shear force. Depending on the type of connection, 3 cases produce, either the connection is full interaction, partial interaction or the connection is negligible. When the shear connecter is of a flexible type and a difference in direct strain at the interface layer result in a slip between the two elements and the difference in deflection sresults in an uplift between the 2 elements.

Roberts (1985) and Al-Amery and Roberts (1990) are assuming that the shear connector is continuous along the length and they are replaced by a layer of negligible thickness having normal and tangential modulus. Yam and Chapman (1968, 1972) is suggesting and developing an approach to incorporate nonlinear material (steel, concrete) and shear connector behavior, the nonlinear differential equation of composite beam had been solved iteratively.

Several previous research are studying fire effect and elevated temperatures on buildings, especially composite beams (Fischer and Varma, 2015, 2017; Jiang *et al*., 2017). Guo (2012) tested the effect of heating and cooling on the composite slabs while Chen *et al.* (2016) studied the effect of elevated temperatures on the shear connectors. The fire or high temperature caused a decrease in the resistance of steel and concrete members and this was confirmed in the composition of the members, butthe amount of the effect of heat here is more difficult to know and the reason that the composite of the member consists of two materials differ in action and a link between them. Heidarpour and Bradford (2010) studied the composite members exposed to high heat but it should be noted that he was assuming of heat in the steel and concrete section change linearly. It should be noted that, the behavior of the steel is different from the concrete as the steel acquires and loses heat quickly while the concrete is acquiring and losing the temperature slowly and the distribution of temperature during the concrete section is nonlinear. Fakury *et al.* (2002) studied the effect of the temperature distribution of composite beam depending on the European standard and found that the temperature rates close to the standard and the largest difference does not exceed 32%.

In this research, we will study the effect of fire and gravity loads on the composite beam. The composite members will be analyzed using a partial interaction approach by the finite elements and for this purpose a program has been built using the language of the Fortran 77.

## MATERIALS AND METHODS

**Finite element idealization:** The finite composite beam has two axes, X, Z for the first material part (steel) and $\bar{X}$

**Corresponding Author:** Muhaned A. Shallal, Department of Civil Engineering, Al-Qadisiyah University, Al Diwaniyah, Iraq

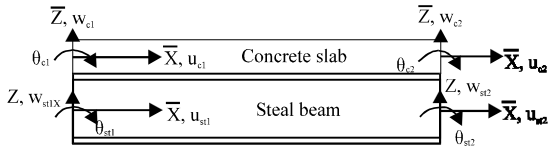


Fig. 1: Displacement components of an element of a composite beam

Table 1: Displacement and strain of materials

| Materials | Displacement (u) |
|---|---|
| Concrete slab | $u_c = u_{oc} - \bar{z}\frac{dw_c}{dx}$ |
| Steel beam | $u_{st} = u_{oct} - z\frac{dw_{st}}{dx}$ |
| Slab reinforcement | $u_{sr} = u_{oc} - dz\frac{dw_c}{dx}$ |
| Strain (ε) | |
| Concrete slab | $\varepsilon_c = \frac{du_{oc}}{dx} - \bar{z}\frac{d^2w_c}{dx^2} = \varepsilon_{oc} - \bar{z}\frac{d^2w_c}{dx^2}$ |
| Steel beam | $\varepsilon_{st} = \frac{du_{ost}}{dx} - Z\frac{d^2w_{st}}{dx^2} = \varepsilon_{ost} - Z\frac{d^2w_c}{dx^2}$ |
| Slab reinforcement | $\varepsilon_c = \frac{du_{oc}}{dx} - dz\frac{d^2w_c}{dx^2} = \varepsilon_{oc} - dz\frac{d^2w_c}{dx^2}$ |

Where: $u_{oc}$ and $u_{ost}$ are central movement in the concrete and steel parts, respectively and $dw_{sr}/dx$ and $dw_c/dx$ are the slopes of steel and concrete parts in z direction, respectively

and $\bar{Z}$ for the second material part (concrete). Each material has two nodes and at each node there are 3 determinants 3 degrees of freedom as shown in Fig. 1, consequently, there are 12 degrees of freedom for each element.

The strain and axial displacement can be found in the terms of deformation w and u relative to the local X and Z axes. From Fig. 2 the strain (ε) and horizontal displacement (u) in each part are listed in Table 1.

The difference in vertical deflection between steel and concrete represents the uplift. The slip, S between the steel and concrete is a difference in the horizontal displacement between steel and concrete at the centerline of the interface (Johnson, 1994):

$$S = u_{oc} - u_{ost} + y_c\frac{dw_c}{dx} + y_s\frac{dw_{st}}{dx} \quad (1)$$

The nodal displacements at each node are:

$$\{d_i\} = \left[u_{sti}\ u_{ci}\ w_{sti}\ w_{ci}\ \theta_{sti}\ u\theta_{ci}\right] \quad (2)$$

Two types of shape function are listed in Eq. 3. The first is a liner shape function (Na) and the second (Nb) is the cubic function (cubic Hermitten) interpolation polynomial:

$$Na = \{N1\ N2\}^T \text{ and } Nb = \left[N3\ N4\ N5\ N6\right]^T \quad (3)$$

Where:

$$Na \rightarrow N1 = 1 - \frac{x}{L} \text{ and } N2 = \frac{x}{L}$$

$$Nb \rightarrow N3 = 1 - \frac{3x^2}{L^2} + \frac{2x^3}{L^3},\ N4 = x - \frac{2x^2}{L} + \frac{x^3}{L^2}$$

$$N5 = \frac{3x^2}{L^2} + \frac{2x^3}{L^3} \text{ and } N6 = -\frac{x^2}{L} + \frac{x^3}{L^2}$$

Using the virtual work principles for beam element under external load:

$$\text{External virtual work} = \int_0^L R_i U_i dx = [R_j]\delta\{d\}^T \quad (4)$$

Where:

$U_i$ = The virtual displacement for nodal displacements
$R_i$ = The applied load
$\{d\}$ = Nodal displacements
$\{R_j\}$ = Equivalent external load

The internal work = summation of internal work in steel section, concrete slab, shear connector and slab reinforcements. Then:

$$[R_j]\{d\} = \int_{\text{Vol. steel}} \delta\varepsilon_{st}\sigma_{st}dvol + \int_{\text{Vol. concrete}} \delta\varepsilon_{st}\sigma_{st}dvol + \sum_{i=1}^{n}\int_O^L \delta \in \varepsilon_{sr}\sigma_{sr}Asrdx + \sum_{m=1}^{ns}\left[q_x\delta S\right]x = xs + \sum_{m=1}^{ns}\left[F_a\delta fa\right]x = xs \quad (5)$$

Where:

$F_a$ = The normal Force (kN), $F_a = f(f_a)$
$q_x$ = The shear force (kN) in x-direction
$n_s$ = The number of shear connectors in each element
n = The number of layer reinforcement
xs = The location of shear connector

The strains expressed as:

$$\left.\begin{aligned} \delta\varepsilon_{st} &= [B_{st}]\delta\{d\} \\ \delta\varepsilon_c &= [B_c]\delta\{d\} \\ \delta\varepsilon_{sr} &= [B_{sr}]\delta\{d\} \\ \delta S &= [B_s]\delta\{d\} \\ \delta F_a &= [B_f]\delta\{d\} \end{aligned}\right\} \quad (6)$$

where, the matrices [B] are the strain-displacement relationship. Combing Eq. 5 and 6 lead to:

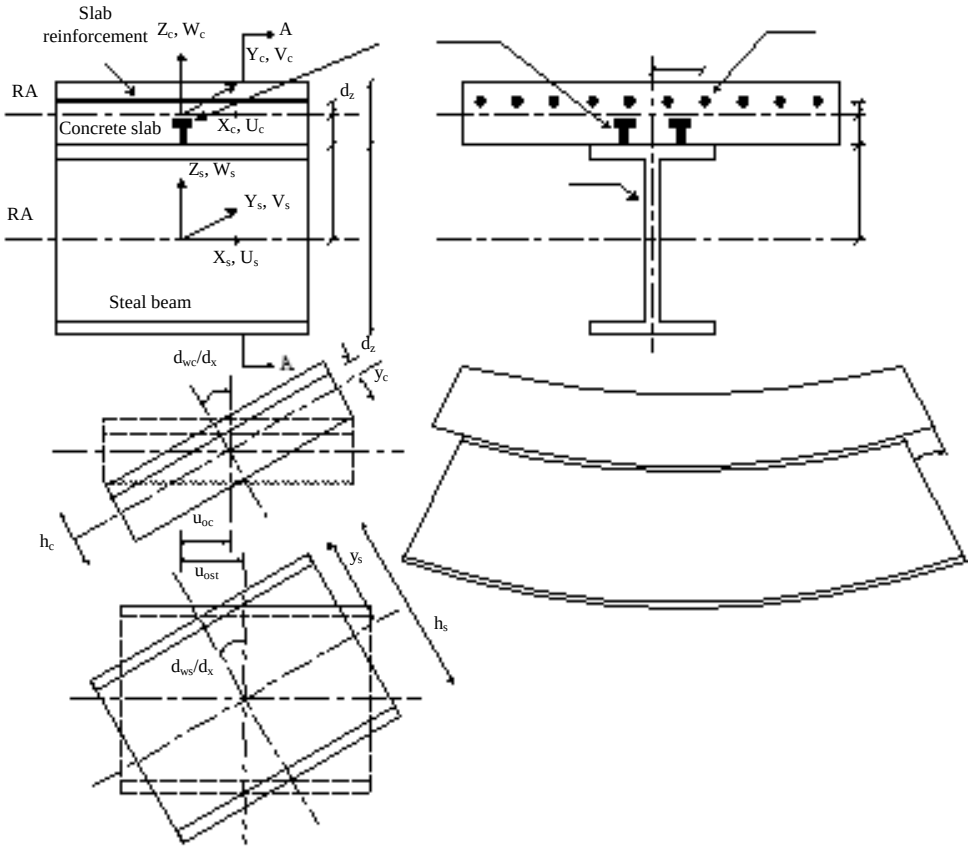


Fig. 2: Deformations of beam segment

$$[R_j]\{d\} = \int_{steel}[B_{st}]^T \sigma_{st} dvol + \int_{concrete}[B_{st}]^T \sigma_c dvol + \sum_{i=1}^{n}\int_O^L [B_{sr}]^T \sigma_{sr} Asr\, dx + \sum_{m=1}^{ns}[B_s]^T qx]_{x=xs} + \sum_{m=1}^{ns}[B_f]^T_{x=xs} \quad (7)$$

and the strain may be written in one column vector $\{\varepsilon\}$ as:

$$\{\varepsilon\} = \begin{Bmatrix} \varepsilon_{st} \\ \varepsilon_c \\ \varepsilon_{sr} \\ S \\ f_a \end{Bmatrix} = \begin{Bmatrix} u_{st1} \\ u_{c1} \\ w_{st1} \\ w_{c1} \\ \theta_{st1} \\ \theta_{c1} \\ u_{st2} \\ u_{c2} \\ w_{st2} \\ w_{c2} \\ \theta_{st2} \\ \theta_{c2} \end{Bmatrix} \quad (8)$$

where, $[B]^T =$

$$\begin{bmatrix} N_1' & 0 & 0 & -N_1 & 0 \\ 0 & N_1' & N_1' & N_1 & 0 \\ -zN_3'' & 0 & 0 & ysN_3' & N_3 \\ 0 & -\bar{z}N_3'' & -dzN_3'' & ycN_3' & -N_3 \\ -zN_4'' & 0 & 0 & ysN_4' & N_4 \\ 0 & -\bar{z}N_4'' & -dzN_4'' & ycN_4' & -N_4 \\ N_2'' & 0 & 0 & -N_2 & 0 \\ 0 & N_2' & N_2' & N2 & 0 \\ -zN_5'' & 0 & 0 & ysN_5' & N_5 \\ 0 & -\bar{z}N_5'' & -dzN_5'' & ycN_5' & -N_5 \\ -zN_6'' & 0 & 0 & ycN_6' & N_6 \\ 0 & -\bar{z}N_6'' & -dzN_6'' & ycN_6' & -N_6 \end{bmatrix}$$

The stiffness matrix of a composite beam element is given by:

$$[K]^e = \int_{vol}[B]^T[D][B]dvol \quad (9)$$

It is composed from the contribution of composite beam components and can be expressed as:

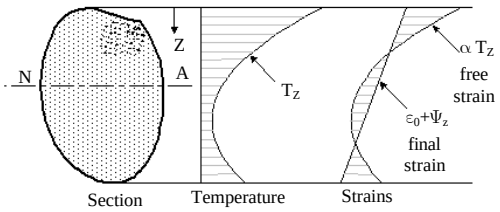


Fig. 3: Thermal strain due to temperature

$$[K]^e = [K]^e_{st} + [K]^e_c + [K]^e_{sr} + [K]^e_s + [K]^e_f \quad (10)$$

Where:

$[K]^e_{st}$ = Steel section element stiffness matrix
$[K]^e_c$ = Concrete slab element stiffness matrix
$[K]^e_{sr}$ = Reinforcement element stiffness matrix
$[K]^e_s$ = Shear connector element stiffness matrix in x-direction
$[K]^e_f$ = Shear connector element stiffness matrix in z-direction

This method of analysis has been used in many researches (Shalall and Louis, 2005; Shallal, 2005).

**Thermal load:** The effect of heat on the structural element depends mainly on the distribution of temperature during the section. There are three types of temperature distribution, the first type is the temperature constant in the structural section and results a longitudinal extension only while the second type of temperature distribution during the section is linear and produces a longitudinal extension and curvature. The third type of temperature distribution is non-linear, this distribution result in longitudinal expansion and curvature as well as stresses called eignstresses.

Figure 3 shows the temperature distribution through generalsection. It should be noted that the study was based on the fact that temperatures are constant at all points that have the same level in z. The free strain profile would be ($\varepsilon_i = \alpha T_z$) where $\alpha$ is the coefficient of thermal expansion. The final strain profile $\varepsilon_z$, shown in Fig. 3 must be linear. The difference between two strains (free and final) produce stresses (eignstresses) equal to:

$$\sigma_z = E(\varepsilon_z - \alpha T_z) \quad (11)$$

where E is the modulus of elasticity. If Eq. 11, integrate produce the axial force (P). Similarly, taking moments of the stress about the neutral axis, the internal moment induced by temperature will be shown in Eq. 13.

$$P = E\iint_A (\varepsilon_z - \alpha T_z)\,dA \quad (12)$$

$$M = E\iint_A (\varepsilon_z - \alpha T_z)\,z\,dA \quad (13)$$

The final strain distribution may be expressed as:

$$\varepsilon_z = \varepsilon_0 - \Psi_z \quad (14)$$

Where:

$\varepsilon_0$ = The final strain at z = 0 (NA)
$\Psi$ = The final curvature.

The final strain at z = 0 and final curvature can be calculated from Eq. 15 and 16:

$$\Psi = \frac{\alpha}{1}\iint_A T_z\,z\,dA \quad (15)$$

$$\varepsilon_0 = \frac{\alpha}{A}\iint_A T_z\,dA \quad (16)$$

Where

A = The section area
I = The second moment of area of the study

In this research, it was assumed that the fire occur below the beam and that the source of heat is from the bottom of the beam. The model that will be used for temperature distribution is shown in Fig. 4a where a constant temperature will be adopted in the steel section, which is equal to the temperature in the concrete surface touching the study while in the concrete section a non-linear. Figure 4b give an example of temperature distribution in concrete thickness equal to 200 mm for other thicknesses (Guo and Shi, 2011) and the details of the temperature distribution are shown in Table 2 for 200 mm and 150 mm.

**Non-linear analysis**

**Material properties at elevated temperature:** In this study, ratio ultimate compressive stress at elevated temperature to ultimate compressive stress that proposed by Shi (1992) is used for concrete in compression, Eq. 11 shows the numerical model of this relation:

$$\frac{fcu^T}{fcu} = \frac{1}{1+\alpha\left(\frac{T}{1000}\right)^b} \quad (17)$$

The coefficients can be taken equal a = 21 and b = 5.7. The stress strain relationship for concrete is suggested by Guo (1999):

Table 2: Temperature value on a concrete section exposed to fire (Guo and Shi, 2011)

| | Concrete thickness (200 mm) | | | | | | | Concrete thickness (150 mm) | | | | | |
|---|---|---|---|---|---|---|---|---|---|---|---|---|---|
| | Time (min) | | | | | | | Time (min) | | | | | |
| h(mm) | 30 | 60 | 90 | 120 | 150 | 180 | h(mm) | 30 | 60 | 90 | 120 | 150 | 180 |
| 200 | 20 | 26 | 42 | 63 | 87 | 110 | 150 | 23 | 51 | 92 | 132 | 169 | 201 |
| 180 | 20 | 28 | 47 | 72 | 99 | 125 | 140 | 23 | 54 | 98 | 141 | 181 | 215 |
| 160 | 21 | 34 | 58 | 88 | 119 | 148 | 120 | 28 | 69 | 120 | 170 | 214 | 253 |
| 140 | 23 | 45 | 78 | 113 | 148 | 181 | 100 | 39 | 97 | 159 | 214 | 263 | 306 |
| 120 | 28 | 64 | 107 | 150 | 189 | 225 | 90 | 49 | 119 | 185 | 244 | 295 | 340 |
| 100 | 39 | 95 | 151 | 200 | 245 | 285 | 80 | 63 | 146 | 218 | 280 | 333 | 380 |
| 90 | 49 | 117 | 179 | 233 | 280 | 321 | 70 | 84 | 180 | 258 | 323 | 378 | 426 |
| 80 | 63 | 145 | 214 | 271 | 320 | 363 | 60 | 112 | 222 | 306 | 374 | 431 | 480 |
| 70 | 84 | 179 | 254 | 316 | 367 | 412 | 50 | 150 | 275 | 364 | 435 | 493 | 543 |
| 60 | 112 | 22 | 304 | 368 | 422 | 468 | 40 | 202 | 341 | 436 | 508 | 566 | 616 |
| 50 | 150 | 275 | 363 | 430 | 486 | 533 | 30 | 273 | 425 | 522 | 595 | 653 | 702 |
| 40 | 202 | 341 | 434 | 504 | 561 | 608 | 20 | 370 | 531 | 629 | 700 | 756 | 803 |
| 30 | 273 | 425 | 512 | 593 | 649 | 696 | 15 | 430 | 594 | 691 | 760 | 814 | 859 |
| 20 | 370 | 530 | 628 | 698 | 753 | 798 | 10 | 504 | 666 | 760 | 826 | 877 | 919 |
| 15 | 432 | 594 | 691 | 759 | 812 | 855 | 5 | 590 | 747 | 836 | 898 | 945 | 983 |
| 10 | 504 | 666 | 760 | 825 | 875 | 916 | 0 | 693 | 839 | 920 | 975 | 1017 | 1050 |
| 5 | 590 | 747 | 836 | 897 | 943 | 981 | | | | | | | |
| 0 | 693 | 839 | 920 | 975 | 1016 | 1049 | | | | | | | |

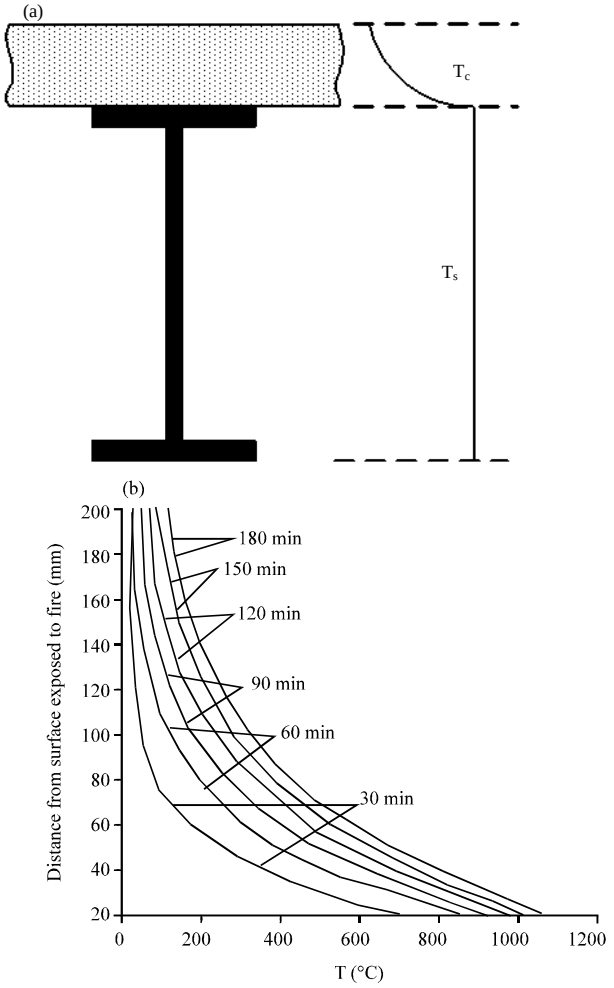


Fig. 4: Model of temperature distribution: a) Composite section and b) Concrete section

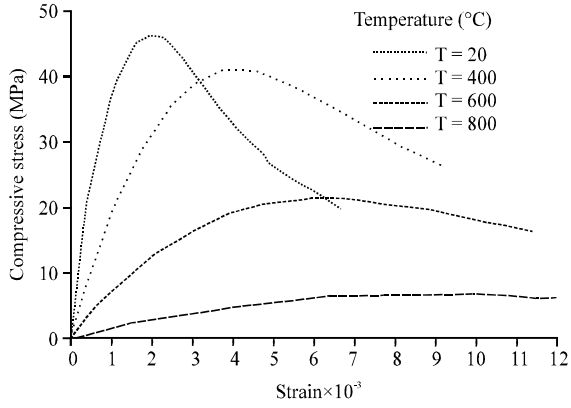


Fig. 5: Stress-strain of concrete at elevated temperature

$$\left.\begin{array}{l} x\le 1.0 \rightarrow y = 2.2x-1.4x^2+0.2x^3 \\ x\le 1.0 \rightarrow \quad y = \dfrac{x}{0.8(x-1)^2+x} \end{array}\right\} \begin{array}{l} y = \dfrac{\sigma}{fc^T} \\ x = \dfrac{\varepsilon}{\varepsilon^T} \end{array} \qquad (18)$$

Where:

$\varepsilon$ and $\sigma$ = The strain and stress of concrete at elevated temperatures, respectively

$fc^T$ and $\varepsilon^T$ = The compressive strength and corresponding peak strain of the concrete

The compressive peak strain of concrete at elevated temperatures increase with the testing temperature. The ratio between it and the value at normal temperatures can be calculated by Eq. 19, Fig. 5 shows the stress-strain of concrete at different temperature:

$$\frac{\varepsilon^T}{\varepsilon} = 1+5\left(\frac{T}{1000}\right)^{1.7} \qquad (19)$$

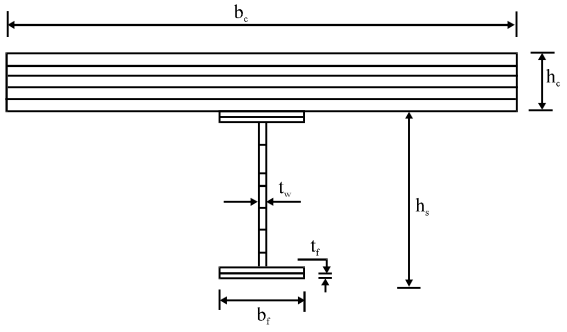


Fig. 6: Layered of composite beam section

Guo and Shi (2011) estimated initial elastic modulus of concrete at elevated temperatures which <700°C:

$$\frac{E^T}{E} = 0.83\text{-}0.0011T \tag{20}$$

The Federation International de la Precontrainte (Anonymous, 1975) suppose the values for the reinforcement under high temperature and simplify according to the corresponding experimental results. The tensile and compressive strengths of reinforcement at elevated temperatures are equal to:

$$\begin{aligned} T \le 200 &\rightarrow \quad fy^T = fy \\ 800 \ge T \ge 200 &\rightarrow fy^T = \left[1\text{-}0.9\left(\frac{T\text{-}200}{600}\right)\right]fy \end{aligned} \tag{21}$$

**Non-linear analysis (cross-section properties):** The modulus of elasticity for each steel and concrete is a function of temperature value at the point under consideration but the temperature varies across the depth of the beam. Beam cross section are divided into a number of layers as shown in Fig. 6, so that:

$$EA = \int_A EdA = \sum_{iL}^{n} E_{iL}A_{iL} \tag{22}$$

$$EA = \int_A Ez^2dA = \sum_{iL}^{n} E_{iL}z^2A_{iL} \tag{23}$$

Where:

n = The number of layers
$E_{iL}$ = The modulus of Elasticity of layer
z = The distance from layer to the reference axis of concrete slab or steel beam
$A_{iL}$ = The cross-sectional Area of the layer

## RESULTS AND DISCUSSION

Two composite beams will be studied to determine the effect of fire. The first beam is examined by Chapman and Balakrishnan (1964) and the second composite beam is an example by Johnson (1994). The dimensions and properties of the two beams are listed in Table 3. Beam No. 2 a was an analysis by Johnson (1994) where it was loaded with a uniform distributed load of 35 kN/m. the maximum sliding was equal to 0.45 mm and is located at the end of the beam. From this analysis, the maximum slip was equal to 0.444 which is located at the end of the beam. From this, we find that the matching is very high and this correlation indicates that the beam is within the limits of perfectly elastic.

Table 3: Properties of study beam

| Simple support beam | No.1 (Chapman and Balakrishnan, 1964) | No.2 (Johnson, 1994) |
|---|---|---|
| Span length | 5.5 m | 10 m |
| External load | Concentrated @ mid span =125 kN | Uniform distributed w = 35 kN/m |
| **Steel beam** | | |
| Steel beam | 305×153 mm | 300×60 (rectangular section) |
| Flange | 153×18.2 mm | |
| Web thickness | 10.16 mm | |
| Young's modulus | 205000 MPa | 200000 MPa |
| Yields stress | 265 MPa | 250 MPa |
| Strain-hardening factor | 0.022 | 0 |
| **Concrete** | | |
| Concrete slab | 1220×153 mm | 600×300 mm |
| cube strength | 50 MPa | 30 MPa |
| Young's modulus | 26700 MPa | 20000 MPa |
| **Shear connector:** | | |
| Diameter | 12.5 mm | 19 mm |
| Height | 50 mm | 100 mm |
| Spacing | 110 mm | 180 mm |
| Number of rows | 2 | 1 |
| Load-slip relation: | Q = 59 (1-EXP (3.1265-$U_{ab}$)) | K = 150 kN/mm |

In this research, we will expose beams to different periods of fire with the normal loads on each beam. Beam No. 1 subjected to concentrated loaded 125kN (one fifth of ultimate load) at the center of the beam while beam No. 2 was loaded with uniform distributed load 35 kN/m. Beams were exposed to periods of 30, 60, 90, 120, 150 and 180 min of fire. Through the analysis, beam No. 2 is collapsed due to the weight exerted on it for a fire period of 3 h.

Figure 7 and 8 illustrate the deflection of the first and second beam, respectively, during different periods of being exposed to fire. Note that with the increase in the duration of the fire increases deflection, this deflection in the early periods with a small increase and more increase in recent periods. The maximum deflectionhas occurredin mid of span for both beams, for beam No. 1 this deflections are equal to 5.24, 6.61, 8.93, 11.75, 15.40, 21.11 and 31.62 mm for fire duration 0, 30, 60, 90, 120, 150 and 180 min, respectively. For beam No. 1 the rate of increase in deflection due to the exposure of fire duration was 126, 170, 224, 294, 403 and 603% of reference deflection. The maximum deflections of beam No. 2 are 24.26, 31.26, 40.90, 53.87, 73.68, 110.73 mm for fire duration 0, 30, 60, 90, 120 and 150 min, respectively. The percent increase in maximum deflections are 129, 168, 220, 304, 456% of reference deflection.

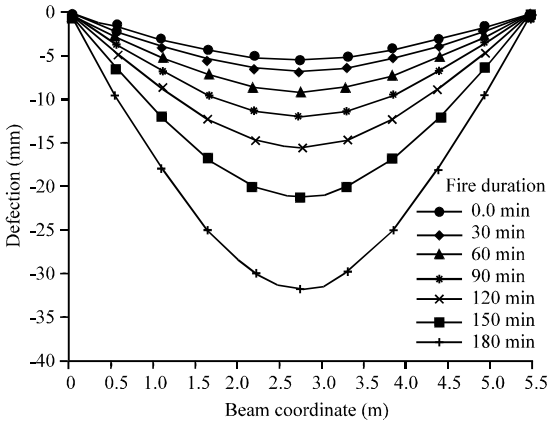


Fig. 7: Deflection curve of beam No. 1 at with different fire duration

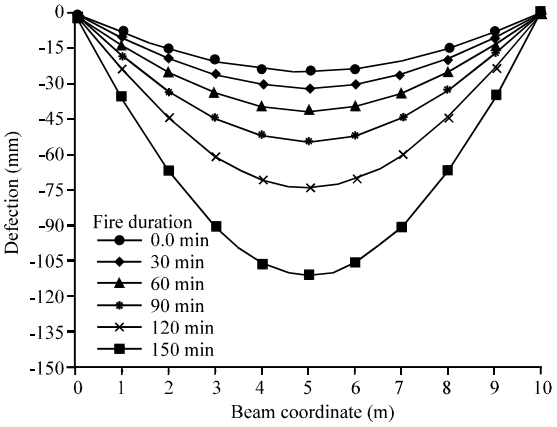


Fig. 8: Deflection curve of beam No. 2 at with different fire duratio

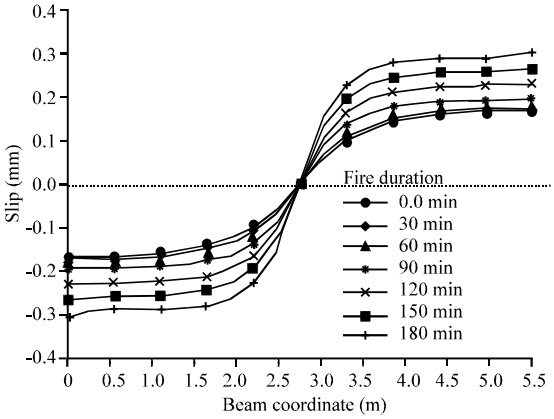


Fig. 9: Slip curve of beam No. 1 at with different fire duration

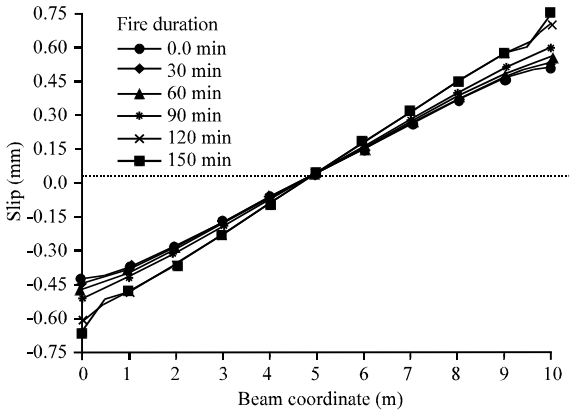


Fig. 10: Slip curve of beam No. 2 at with different fire duration

Figure 9 and 10 illustrate the slip between the steel section and the concrete slab of thestudentmodels for different periods of exposure of beams to fires. By observing, the two figures, we find that the amount of slip is zero in the middle of the beam and the largest value at the end and these results are consistent with previous studies of composite beams.

The maximum slip in the first model was 0.168, 0.172, 0.18, 0.194, 0.229, 0.265 and 0.304 mm when the model was subjected to periods of fire duration equal to 0, 30, 60, 90, 120, 150 and 180 min, respectively. The increase in slip relative to the model that did not subject to fire was 102, 108, 116, 136, 158 and 181% for fire duration 0, 30, 60, 90, 120, 150 and 180 min, respectively.

In the second beam, the maximum slip values were 0.444, 0.461, 0.49, 0.53, 0.629 and 0.673 mm for fire duration equal to 0, 30, 60, 90, 120 and 150 min. The increase in slip was 104, 110, 119, 142 and 152% of the reference beam.

## CONCLUSION

The research focused is the study of the effect of fire and normal loads on the composite members (steel and concrete). Through the study, showing one of the models (Beam No. 2) has collapsed for a fire duration reached 180 min. The effect of the fire was clear and noticeable on the deflection in the beams. The amount of increase in deflection reached 603% for the first beam when it was subject to 180 min. of fire while the second model was the percentage of increase in deflection reached to 456% when exposed to fire duration reached to 150 min. The fire effect on slip was less severe than the effect on deflection and the largest increase in slip 181 and 152% for the first and second beam, respectively.

## REFERENCES

Al-Amery, R.I.M. and T.M. Roberts, 1990. Nonlinear finite difference analysis of composite beams with partial interaction. Comput. Struct., 35: 81-87.

Anonymous, 1975. Recommendations for the design of reinforced and prestressed concrete structural members for fire resistance. Federation International de la Precontrainte (FIP), Amsterdam, the Netherlands.

Chapman, J.C. and S. Balakrishnan, 1964. Experiments on composite beams. Struct. Eng., 42: 369-383.

Chen, L.Z., G. Ranzi, S.C. Jiang, F. Tahmasebinia and G.Q. Li, 2016. Performance and design of shear connectors in composite beams with parallel profiled sheeting at elevated temperatures. Intl. J. Steel Struct., 16: 217-229.

Fakury, R.H., E.B. De Las Casas, F.P.F. Junior and L.M.P. De Abreu, 2002. Numerical Analysis of the Eurocode Assumptions for Temperature Distribution in Composite Steel and Concrete Beams. In: Mecanica Computacional, Idelsohn, S.R., V.E. Sonzogni and A. Cardona (Eds.). Asociacion Argentina de Mecanica Computacional, Santa Fe, Argentina, pp: 1998-2008.

Fischer, E.C. and A.H. Varma, 2015. Fire behavior of composite beams with simple connections: Benchmarking of numerical models. J. Constr. Steel Res., 111: 112-125.

Fischer, E.C. and A.H. Varma, 2017. Fire resilience of composite beams with simple connections: Parametric studies and design. J. Constr. Steel Res., 128: 119-135.

Guo, S., 2012. Experimental and numerical study on restrained composite slab during heating and cooling. J. Constr. Steel Res., 69: 95-105.

Guo, Z. and X. Shi, 2011. Experiment and Calculation of Reinforced Concrete at Elevated Temperatures. Elsevier, New York, USA., ISBN:978-0-12-386962-3, Pages: 312.

Guo, Z., 1999. The Principle of Reinforced Concrete. Tsinghua University Press, Beijing, China,.

Heidarpour, A. and M.A. Bradford, 2010. Nonlinear analysis of composite beams with partial interaction in steel frame structures at elevated temperature. J. Struct. Eng., 136: 968-977.

Jiang, S.C., G. Ranzi, L.Z. Chen and G.Q. Li, 2017. Behaviour and design of composite beams with composite slabs at elevated temperatures. Adv. Struct. Eng., 20: 1451-1465.

Johnson, R.P., 1994. Composite Structures of Steel and Concrete, Beams, Columns, Frames. Wiley-Blackwell, Hoboken, New Jersey, USA.,.

Roberts, T.M., 1985. Finite difference analysis of composite beams with partial interaction. Comput. Struct., 21: 469-473.

Shalall, M.A. and M.A. Louis, 2005. Non-linear analysis of simply supported composite beam by finite element method. J. Eng. Dev., 9: 8-22.

Shallal, M.A., 2005. Nonlinear analysis of continuous composite beam by finite element method. J. Eng. Sustain. Dev., 9: 54-69.

Shi, X., 1992. Experimental investigation and non-linear finite element analysis of reinforced concrete beam-column structures under loading and elevated temperature. Ph.D Thesis, Tsinghua University, Beijing, China.

Yam, L.C.P. and J.C. Chapman, 1968. The inelastic behaviour of simply supported composite beams of steel and concrete. Proc. Inst. Civil Eng., 41: 651-683.

Yam, L.C.P. and J.C. Chapman, 1972. The inelastic behavior of continuous composite beams of steel and concrete. Inst. Civil Eng. Pt2 Res. Theor., 53: 487-501.